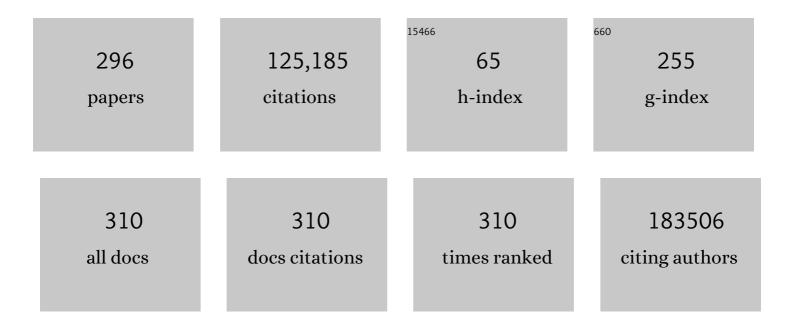
List of Publications by Year in descending order

Source: https://exaly.com/author-pdf/1762642/publications.pdf Version: 2024-02-01



#	Article	IF	CITATIONS
1	2020 Biolmage Analysis Survey: Community experiences and needs for the future. Biological Imaging, 2022, 1, .	1.0	15
2	Meeting in the Middle: Towards Successful Multidisciplinary Bioimage Analysis Collaboration. Frontiers in Bioinformatics, 2022, 2, .	1.0	3
3	A Model of Discovery: The Role of Imaging Established and Emerging Non-mammalian Models in Neuroscience. Frontiers in Molecular Neuroscience, 2022, 15, 867010.	1.4	3
4	HIV RGB: Automated Single-Cell Analysis of HIV-1 Rev-Dependent RNA Nuclear Export and Translation Using Image Processing in KNIME. Viruses, 2022, 14, 903.	1.5	1
5	The <scp>ImageJ</scp> ecosystem: Openâ€source software for image visualization, processing, and analysis. Protein Science, 2021, 30, 234-249.	3.1	102
6	Evaluating the effectiveness of a lower extremity venous phantom on developing ultrasound examination skills and confidence. Ultrasound, 2021, 29, 18-26.	0.3	2
7	Collagen Organization in Relation to Ductal Carcinoma <i>In Situ</i> Pathology and Outcomes. Cancer Epidemiology Biomarkers and Prevention, 2021, 30, 80-88.	1.1	21
8	Modeling early thermal injury using an ex vivo human skin model of contact burns. Burns, 2021, 47, 611-620.	1.1	12
9	Response to letter to the editor on "The use of human ex vivo models in burn research – Developments and perspectives― Burns, 2021, 47, 968-969.	1.1	1
10	Single image super-resolution for whole slide image using convolutional neural networks and self-supervised color normalization. Medical Image Analysis, 2021, 68, 101938.	7.0	25
11	Microstructure and resident cell-types of the feline optic nerve head resemble that of humans. Experimental Eye Research, 2021, 202, 108315.	1.2	9
12	Challenges of conducting quantitative ultrasound with a multimodal optical imaging system. Physics in Medicine and Biology, 2021, 66, 035008.	1.6	1
13	Navigating the Collagen Jungle: The Biomedical Potential of Fiber Organization in Cancer. Bioengineering, 2021, 8, 17.	1.6	42
14	Harnessing non-destructive 3D pathology. Nature Biomedical Engineering, 2021, 5, 203-218.	11.6	74
15	Hyperdimensional Imaging Contrast Using an Optical Fiber. Sensors, 2021, 21, 1201.	2.1	2
16	Cultured cardiac fibroblasts and myofibroblasts express Sushi Containing Domain 2 and assemble a unique fibronectin rich matrix. Experimental Cell Research, 2021, 399, 112489.	1.2	4
17	Pycro-Manager: open-source software for customized and reproducible microscope control. Nature Methods, 2021, 18, 226-228.	9.0	54
18	Ellipsoid Zone Defects in Retinal Vein Occlusion Correlates With Visual Acuity Prognosis: SCORE2 Report 14. Translational Vision Science and Technology, 2021, 10, 31.	1.1	12

#	Article	IF	CITATIONS
19	A device for the controlled cooling and freezing of excised plant specimens during magnetic resonance imaging. Plant Methods, 2021, 17, 41.	1.9	5
20	Hyperpolarized 13C Magnetic Resonance Spectroscopic Imaging of Pyruvate Metabolism in Murine Breast Cancer Models of Different Metastatic Potential. Metabolites, 2021, 11, 274.	1.3	8
21	Open-source deep-learning software for bioimage segmentation. Molecular Biology of the Cell, 2021, 32, 823-829.	0.9	50
22	Developing open-source software for bioimage analysis: opportunities and challenges. F1000Research, 2021, 10, 302.	0.8	20
23	Joint regression-classification deep learning framework for analyzing fluorescence lifetime images using NADH and FAD. Biomedical Optics Express, 2021, 12, 2703.	1.5	8
24	ImageJ and CellProfiler: Complements in Open‧ource Bioimage Analysis. Current Protocols, 2021, 1, e89.	1.3	20
25	Rhesus monkeys as a translational model for lateâ€onset Alzheimer's disease. Aging Cell, 2021, 20, e13374.	3.0	10
26	New Extensibility and Scripting Tools in the ImageJ Ecosystem. Current Protocols, 2021, 1, e204.	1.3	3
27	Real-time polarization microscopy of fibrillar collagen in histopathology. Scientific Reports, 2021, 11, 19063.	1.6	12
28	Open source remote monitoring of research lasers. Optics and Laser Technology, 2021, 143, 107363.	2.2	0
29	Measuring the spatial distribution of multiply scattered light using a de-scanned image sensor for examining retinal structure contrast. Optics Express, 2021, 29, 552.	1.7	2
30	Structured Correlation Detection with Application to Colocalization Analysis in Dual-Channel Fluorescence Microscopic Imaging. Statistica Sinica, 2021, 31, 333-360.	0.2	4
31	Introduction to the Biophotonics Congress 2020 feature issue. Biomedical Optics Express, 2021, 12, 509.	1.5	0
32	Dual-stream Multiple Instance Learning Network for Whole Slide Image Classification with Self-supervised Contrastive Learning. , 2021, 2021, 14318-14328.		216
33	Mammary collagen architecture and its association with mammographic density and lesion severity among women undergoing image-guided breast biopsy. Breast Cancer Research, 2021, 23, 105.	2.2	17
34	Machine Learning Methods for Fluorescence Lifetime Imaging (FLIM) Based Label-Free Detection of Microglia. Frontiers in Neuroscience, 2020, 14, 931.	1.4	24
35	Evolution of ischemia and neovascularization in a murine model of full thickness human wound healing. Wound Repair and Regeneration, 2020, 28, 812-822.	1.5	8
36	Distinct Tissue Damage and Microbial Cues Drive Neutrophil and Macrophage Recruitment to Thermal Injury. IScience, 2020, 23, 101699.	1.9	13

#	Article	IF	CITATIONS
37	Second Harmonic Generation Imaging of Collagen in Chronically Implantable Electrodes in Brain Tissue. Frontiers in Neuroscience, 2020, 14, 95.	1.4	14
38	Non-disruptive collagen characterization in clinical histopathology using cross-modality image synthesis. Communications Biology, 2020, 3, 414.	2.0	23
39	Optical imaging of collagen fiber damage to assess thermally injured human skin. Wound Repair and Regeneration, 2020, 28, 848-855.	1.5	15
40	3-D-Printed Registration Phantom for Combined Ultrasound and Optical Imaging of Biological Tissues. Ultrasound in Medicine and Biology, 2020, 46, 1808-1814.	0.7	3
41	Abstract 18: Augmentation of the Wisconsin "Blue-Blood―Chicken Thigh Model with Fluorescent Imaging Enhances the Assessment of Anastomotic Patency in Supermicrosurgical Training. Plastic and Reconstructive Surgery - Global Open, 2020, 8, 10-11.	0.3	0
42	A syringe adapter for reduced muscular strain and fatigue. Applied Ergonomics, 2020, 85, 103061.	1.7	3
43	Molecular and Functional Networks Linked to Sarcopenia Prevention by Caloric Restriction in Rhesus Monkeys. Cell Systems, 2020, 10, 156-168.e5.	2.9	31
44	Fibrillar Collagen Quantification With Curvelet Transform Based Computational Methods. Frontiers in Bioengineering and Biotechnology, 2020, 8, 198.	2.0	32
45	Integration of the ImageJ Ecosystem in KNIME Analytics Platform. Frontiers in Computer Science, 2020, 2, .	1.7	24
46	A semi-automated machine-learning based workflow for ellipsoid zone analysis in eyes with macular edema: SCORE2 pilot study. PLoS ONE, 2020, 15, e0232494.	1.1	9
47	Recovery and Regrowth After Nerve Repair: A Systematic Analysis of Four Repair Techniques. Journal of Surgical Research, 2020, 251, 311-320.	0.8	5
48	Citrullination regulates wound responses and tissue regeneration in zebrafish. Journal of Cell Biology, 2020, 219, .	2.3	9
49	Metabolic mapping of glioblastoma stem cells reveals NADH fluxes associated with glioblastoma phenotype and survival. Journal of Biomedical Optics, 2020, 25, 1.	1.4	8
50	Microglia activation visualization via fluorescence lifetime imaging microscopy of intrinsically fluorescent metabolic cofactors. Neurophotonics, 2020, 7, 1.	1.7	8
51	Intensity-based registration of bright-field and second-harmonic generation images of histopathology tissue sections. Biomedical Optics Express, 2020, 11, 160.	1.5	19
52	Quantitative phase imaging of stromal prognostic markers in pancreatic ductal adenocarcinoma. Biomedical Optics Express, 2020, 11, 1354.	1.5	22
53	Platform for quantitative multiscale imaging of tissue composition. Biomedical Optics Express, 2020, 11, 1927.	1.5	3
54	Parallel multiphoton excited fabrication of tissue engineering scaffolds using a diffractive optical element. Optics Express, 2020, 28, 2744.	1.7	4

#	Article	IF	CITATIONS
55	FLIMJ: An open-source ImageJ toolkit for fluorescence lifetime image data analysis. PLoS ONE, 2020, 15, e0238327.	1.1	23
56	Drosophila TRIM32 cooperates with glycolytic enzymes to promote cell growth. ELife, 2020, 9, .	2.8	24
57	Fluorescence Anisotropy in Autofluorescence Imaging and Metabolic Interpretations. , 2020, , .		Ο
58	Quantifying Fibrillar Collagen Organization with Curvelet Transform-Based Tools. Journal of Visualized Experiments, 2020, , .	0.2	7
59	FLIMJ: An open-source ImageJ toolkit for fluorescence lifetime image data analysis. , 2020, 15, e0238327.		0
60	FLIMJ: An open-source ImageJ toolkit for fluorescence lifetime image data analysis. , 2020, 15, e0238327.		0
61	FLIMJ: An open-source ImageJ toolkit for fluorescence lifetime image data analysis. , 2020, 15, e0238327.		0
62	FLIMJ: An open-source ImageJ toolkit for fluorescence lifetime image data analysis. , 2020, 15, e0238327.		0
63	A Novel Anisotropy Imaging Technique for NAD(P)H Autofluorescence. Microscopy and Microanalysis, 2019, 25, 1246-1247.	0.2	3
64	ImageJ for the Next Generation of Scientific Image Data. Microscopy and Microanalysis, 2019, 25, 142-143.	0.2	21
65	An Investigation Into the Challenges of Using Metal Additive Manufacturing for the Production of Patient-Specific Aneurysm Clips. Journal of Medical Devices, Transactions of the ASME, 2019, 13, .	0.4	1
66	Mammographic Density: Intersection of Advocacy, Science, and Clinical Practice. Current Breast Cancer Reports, 2019, 11, 100-110.	0.5	1
67	PGCâ€l a integrates a metabolism and growth network linked to caloric restriction. Aging Cell, 2019, 18, e12999.	3.0	25
68	Quantitative Histopathology of Stained Tissues using Color Spatial Light Interference Microscopy (cSLIM). Scientific Reports, 2019, 9, 14679.	1.6	30
69	NAD(P)H fluorescence lifetime measurements in fixed biological tissues. Methods and Applications in Fluorescence, 2019, 7, 044005.	1.1	22
70	Shedding Light. , 2019, , .		2
71	Quantitative second harmonic generation imaging of leporine, canine, and porcine vocal fold collagen. Laryngoscope, 2019, 129, 2549-2556.	1.1	0
72	Transglutaminase-2 Mediates the Biomechanical Properties of the Colorectal Cancer Tissue Microenvironment that Contribute to Disease Progression. Cancers, 2019, 11, 701.	1.7	12

#	Article	IF	CITATIONS
73	A multiscale Mueller polarimetry module for a stereo zoom microscope. Biomedical Engineering Letters, 2019, 9, 339-349.	2.1	8
74	Scientific Community Image Forum: A discussion forum for scientific image software. PLoS Biology, 2019, 17, e3000340.	2.6	27
75	Coding Scheme Optimization for Fast Fluorescence Lifetime Imaging. ACM Transactions on Graphics, 2019, 38, 1-16.	4.9	3
76	Collagen organization of renal cell carcinoma differs between low and high grade tumors. BMC Cancer, 2019, 19, 490.	1.1	41
77	Spatially Adaptive Colocalization Analysis in Dual-Color Fluorescence Microscopy. IEEE Transactions on Image Processing, 2019, 28, 4471-4485.	6.0	10
78	Cortex-wide neural interfacing via transparent polymer skulls. Nature Communications, 2019, 10, 1500.	5.8	71
79	Optimization of interstrand interactions enables burn detection with a collagen-mimetic peptide. Organic and Biomolecular Chemistry, 2019, 17, 9906-9912.	1.5	19
80	A novel bioreactor for combined magnetic resonance spectroscopy and optical imaging of metabolism in 3D cell cultures. Magnetic Resonance in Medicine, 2019, 81, 3379-3391.	1.9	12
81	Impact of tissue preservation on collagen fiber architecture. Biotechnic and Histochemistry, 2019, 94, 134-144.	0.7	8
82	Autofluorescence lifetime imaging of cellular metabolism: Sensitivity toward cell density, pH, intracellular, and intercellular heterogeneity. Cytometry Part A: the Journal of the International Society for Analytical Cytology, 2019, 95, 56-69.	1.1	46
83	Super-resolution recurrent convolutional neural networks for learning with multi-resolution whole slide images. Journal of Biomedical Optics, 2019, 24, 1.	1.4	12
84	Optical fiber-based dispersion for spectral discrimination in fluorescence lifetime imaging systems. Journal of Biomedical Optics, 2019, 25, 1.	1.4	2
85	Nonparametric empirical Bayesian framework for fluorescence-lifetime imaging microscopy. Biomedical Optics Express, 2019, 10, 5497.	1.5	19
86	Distinct inflammatory and wound healing responses to complex caudal fin injuries of larval zebrafish. ELife, 2019, 8, .	2.8	72
87	Fluorescence lifetime-based intrinsic metabolic signatures of microglia cell (Conference) Tj ETQq1 1 0.784314	4 rgBT /Overl	ock_10 Tf 50
88	Automated and Robust Quantification of Colocalization in Dual-Color Fluorescence Microscopy: A Nonparametric Statistical Approach. IEEE Transactions on Image Processing, 2018, 27, 622-636.	6.0	11
89	The Presence of Cyclooxygenase 2, Tumor-Associated Macrophages, and Collagen Alignment as Prognostic Markers for Invasive Breast Carcinoma Patients. American Journal of Pathology, 2018, 188, 559-573.	1.9	75
90	An open source, 3D printed preclinical MRI phantom for repeated measures of contrast agents and reference standards. Biomedical Physics and Engineering Express, 2018, 4, 027005.	0.6	4

#	Article	IF	CITATIONS
91	Collagen Alignment as a Predictor of Recurrence after Ductal Carcinoma <i>In Situ</i> . Cancer Epidemiology Biomarkers and Prevention, 2018, 27, 138-145.	1.1	94
92	Convolutional neural networks for whole slide image superresolution. Biomedical Optics Express, 2018, 9, 5368.	1.5	13
93	Imaging the Cardiac Extracellular Matrix. Advances in Experimental Medicine and Biology, 2018, 1098, 21-44.	0.8	12
94	Targeted matrisome analysis identifies thrombospondin-2 and tenascin-C in aligned collagen stroma from invasive breast carcinoma. Scientific Reports, 2018, 8, 12941.	1.6	51
95	FunImageJ: a Lisp framework for scientific image processing. Bioinformatics, 2018, 34, 899-900.	1.8	7
96	GSK3β Regulates Brain Energy Metabolism. Cell Reports, 2018, 23, 1922-1931.e4.	2.9	55
97	Imaging Vacuolar Anthocyanins with Fluorescence Lifetime Microscopy (FLIM). Methods in Molecular Biology, 2018, 1789, 131-141.	0.4	3
98	Damage-induced reactive oxygen species regulate vimentin and dynamic collagen-based projections to mediate wound repair. ELife, 2018, 7, .	2.8	57
99	Chemically Derived Kirigami of WSe ₂ . Journal of the American Chemical Society, 2018, 140, 10980-10987.	6.6	33
100	Syndecan-1 induction in lung microenvironment supports the establishment of breast tumor metastases. Breast Cancer Research, 2018, 20, 66.	2.2	35
101	Void spot assay procedural optimization and software for rapid and objective quantification of rodent voiding function, including overlapping urine spots. American Journal of Physiology - Renal Physiology, 2018, 315, F1067-F1080.	1.3	37
102	Neighborhood regularized image superresolution for applications to microscopic imaging. , 2018, , .		1
103	Changes in Cutaneous Gene Expression after Microvascular Free Tissue Transfer in Parry-Romberg Syndrome. Plastic and Reconstructive Surgery, 2018, 142, 303e-309e.	0.7	12
104	Review of quantitative multiscale imaging of breast cancer. Journal of Medical Imaging, 2018, 5, 1.	0.8	14
105	Abstract 3598: Classification of the collagen ECM in normal human tissue as a biomarker for future breast cancer incidence. , 2018, , .		0
106	ImageJ-MATLAB: a bidirectional framework for scientific image analysis interoperability. Bioinformatics, 2017, 33, 629-630.	1.8	35
107	Neuroendocrine Tumorâ€Targeted Upconversion Nanoparticleâ€Based Micelles for Simultaneous NIRâ€Controlled Combination Chemotherapy and Photodynamic Therapy, and Fluorescence Imaging. Advanced Functional Materials, 2017, 27, 1604671.	7.8	138
108	Beyond the margins: real-time detection of cancer using targeted fluorophores. Nature Reviews Clinical Oncology, 2017, 14, 347-364.	12.5	366

#	Article	IF	CITATIONS
109	Elevated collagen-I augments tumor progressive signals, intravasation and metastasis of prolactin-induced estrogen receptor alpha positive mammary tumor cells. Breast Cancer Research, 2017, 19, 9.	2.2	104
110	Aging and caloric restriction impact adipose tissue, adiponectin, and circulating lipids. Aging Cell, 2017, 16, 497-507.	3.0	94
111	Enriching Islet Phospholipids With Eicosapentaenoic Acid Reduces Prostaglandin E2 Signaling and Enhances Diabetic β-Cell Function. Diabetes, 2017, 66, 1572-1585.	0.3	41
112	Complex and Noncentrosymmetric Stacking of Layered Metal Dichalcogenide Materials Created by Screw Dislocations. Journal of the American Chemical Society, 2017, 139, 3496-3504.	6.6	81
113	Stromal alterations in ovarian cancers via wavelength dependent Second Harmonic Generation microscopy and optical scattering. BMC Cancer, 2017, 17, 102.	1.1	27
114	Wavelength dependent SHG imaging and scattering probes of extracellular matrix (ECM) alterations in ovarian cancer (Conference Presentation). , 2017, , .		0
115	Quantitating the cell: turning images into numbers with <scp>ImageJ</scp> . Wiley Interdisciplinary Reviews: Developmental Biology, 2017, 6, e260.	5.9	108
116	Selected mitochondrial DNA landscapes activate the SIRT3 axis of the UPRmt to promote metastasis. Oncogene, 2017, 36, 4393-4404.	2.6	78
117	Trainable Weka Segmentation: a machine learning tool for microscopy pixel classification. Bioinformatics, 2017, 33, 2424-2426.	1.8	1,505
118	Fabrication approaches for the creation of physical models from microscopy data. 3D Printing in Medicine, 2017, 3, 2.	1.7	1
119	Diverse activities of viralcis-acting RNA regulatory elements revealed using multicolor, long-term, single-cell imaging. Molecular Biology of the Cell, 2017, 28, 476-487.	0.9	10
120	<scp>SHARPIN</scp> regulates collagen architecture and ductal outgrowth in the developing mouse mammary gland. EMBO Journal, 2017, 36, 165-182.	3.5	39
121	Design of an Open-Source Binary Micromultileaf Collimator for a Small Animal Microradiotherapy System. Journal of Medical Devices, Transactions of the ASME, 2017, 11, .	0.4	1
122	Methods for Quantifying Fibrillar Collagen Alignment. Methods in Molecular Biology, 2017, 1627, 429-451.	0.4	115
123	Fluorescence of Picrosirius Red Multiplexed With Immunohistochemistry for the Quantitative Assessment of Collagen in Tissue Sections. Journal of Histochemistry and Cytochemistry, 2017, 65, 479-490.	1.3	78
124	Quantification of Collagen Organization after Nerve Repair. Plastic and Reconstructive Surgery - Global Open, 2017, 5, e1586.	0.3	10
125	Long-term Live Imaging Device for Improved Experimental Manipulation of Zebrafish Larvae. Journal of Visualized Experiments, 2017, , .	0.2	6
126	A beam optics study of a modular multi-source X-ray tube for novel computed tomography applications. Nuclear Instruments and Methods in Physics Research, Section A: Accelerators, Spectrometers, Detectors and Associated Equipment, 2017, 868, 1-9.	0.7	13

#	Article	IF	CITATIONS
127	zWEDGI: Wounding and Entrapment Device for Imaging Live Zebrafish Larvae. Zebrafish, 2017, 14, 42-50.	0.5	31
128	TrackMate: An open and extensible platform for single-particle tracking. Methods, 2017, 115, 80-90.	1.9	2,546
129	Administration of Non-Torsadogenic human Ether-Ã-go-go-Related Gene Inhibitors Is Associated with Better Survival for High hERG–Expressing Glioblastoma Patients. Clinical Cancer Research, 2017, 23, 73-80.	3.2	40
130	3D second harmonic generation imaging tomography by multi-view excitation. Optica, 2017, 4, 1171.	4.8	16
131	Quantification of collagen organization in histopathology samples using liquid crystal based polarization microscopy. Biomedical Optics Express, 2017, 8, 4243.	1.5	39
132	The Kinesin Adaptor Calsyntenin-1 Organizes Microtubule Polarity and Regulates Dynamics during Sensory Axon Arbor Development. Frontiers in Cellular Neuroscience, 2017, 11, 107.	1.8	31
133	ImageJ2: ImageJ for the next generation of scientific image data. BMC Bioinformatics, 2017, 18, 529.	1.2	4,464
134	Thermal Conductivity Measurement of Granular UO ₂ (NO ₃) ₂ · 6H ₂ O. Nuclear Technology, 2017, 197, 191-200.	0.7	0
135	The ImageJ Ecosystem: An Open and Extensible Platform for Biomedical Image Analysis Microscopy and Microanalysis, 2017, 23, 226-227.	0.2	12
136	Abstract TMEM-015: QUANTITATIVE ASSESSMENT OF THE ROLE OF COLLAGEN ALTERATIONS IN OVARIAN CANCER. , 2017, , .		0
137	Calcific Aortic Valve Disease Is Associated with Layer-Specific Alterations in Collagen Architecture. PLoS ONE, 2016, 11, e0163858.	1.1	50
138	Blue Light Modulates Murine Microglial Gene Expression in the Absence of Optogenetic Protein Expression. Scientific Reports, 2016, 6, 21172.	1.6	36
139	In Vivo Visualization of Stromal Macrophages via label-free FLIM-based metabolite imaging. Scientific Reports, 2016, 6, 25086.	1.6	65
140	NAD(P)H-FLIM and FRET Imaging of Pancreatic Islet Oscillations Reveals Novel Activators of Mitochondrial Respiratory Complex I in the Setting of Obesity. Biophysical Journal, 2016, 110, 486a-487a.	0.2	0
141	Membrane dynamics during cellular wound repair. Molecular Biology of the Cell, 2016, 27, 2272-2285.	0.9	87
142	Mechanical signals regulate and activate SNAIL1 protein to control the fibrogenic response of CAFs. Journal of Cell Science, 2016, 129, 1989-2002.	1.2	57
143	Validation of an arterial constitutive model accounting for collagen content and crosslinking. Acta Biomaterialia, 2016, 31, 276-287.	4.1	22
144	Association of collagen architecture with glioblastoma patient survival. Journal of Neurosurgery, 2016, 126, 1812-1821.	0.9	78

#	Article	IF	CITATIONS
145	Advanced quantitative imaging and biomechanical analyses of periosteal fibers in accelerated bone growth. Bone, 2016, 92, 201-213.	1.4	5
146	Radiation Promptly Alters Cancer Live Cell Metabolic Fluxes: An In Vitro Demonstration. Radiation Research, 2016, 185, 496.	0.7	5
147	Using fluorescence lifetime microscopy to study the subcellular localization of anthocyanins. Plant Journal, 2016, 88, 895-903.	2.8	19
148	Comparison of Picrosirius Red Staining With Second Harmonic Generation Imaging for the Quantification of Clinically Relevant Collagen Fiber Features in Histopathology Samples. Journal of Histochemistry and Cytochemistry, 2016, 64, 519-529.	1.3	68
149	Expression of the <i>Drosophila</i> homeobox gene, <i>Distalâ€less</i> , supports an ancestral role in neural development. Developmental Dynamics, 2016, 245, 87-95.	0.8	9
150	3D texture analysis for classification of second harmonic generation images of human ovarian cancer. Scientific Reports, 2016, 6, 35734.	1.6	51
151	Human pancreatic stellate cells modulate 3D collagen alignment to promote the migration of pancreatic ductal adenocarcinoma cells. Biomedical Microdevices, 2016, 18, 105.	1.4	33
152	ImageJ: Image Analysis Interoperability for the Next Generation of Biological Image Data. Microscopy and Microanalysis, 2016, 22, 2066-2067.	0.2	3
153	Lactation opposes pappalysinâ€1â€driven pregnancyâ€associated breast cancer. EMBO Molecular Medicine, 2016, 8, 388-406.	3.3	41
154	SCIFIO: an extensible framework to support scientific image formats. BMC Bioinformatics, 2016, 17, 521.	1.2	25
155	Preparation of 3D Collagen Gels and Microchannels for the Study of 3D Interactions In Vivo . Journal of Visualized Experiments, 2016, , .	0.2	10
156	Charcot-Marie-Tooth 2b associated Rab7 mutations cause axon growth and guidance defects during vertebrate sensory neuron development. Neural Development, 2016, 11, 2.	1.1	43
157	The Action of Discoidin Domain Receptor 2 in Basal Tumor Cells and Stromal Cancer-Associated Fibroblasts Is Critical for Breast Cancer Metastasis. Cell Reports, 2016, 15, 2510-2523.	2.9	85
158	TUDCA Rescues Î ³ -Cell Metabolic Oscillations from ER Stress, Revealed By NAD(P)H-FLIM and FRET. Biophysical Journal, 2016, 110, 142a-143a.	0.2	0
159	Pancreatic β-Cells From Mice Offset Age-Associated Mitochondrial Deficiency With Reduced KATP Channel Activity. Diabetes, 2016, 65, 2700-2710.	0.3	59
160	Regional metabolic heterogeneity of the hippocampus is nonuniformly impacted by age and caloric restriction. Aging Cell, 2016, 15, 100-110.	3.0	27
161	Lineage Reprogramming of Fibroblasts into Proliferative Induced Cardiac Progenitor Cells by Defined Factors. Cell Stem Cell, 2016, 18, 354-367.	5.2	165
162	Advanced Intestinal Cancers often Maintain a Multi-Ancestral Architecture. PLoS ONE, 2016, 11, e0150170.	1.1	5

#	Article	IF	CITATIONS
163	Induction of fibroblast senescence generates a non-fibrogenic myofibroblast phenotype that differentially impacts on cancer prognosis. Aging, 2016, 9, 114-132.	1.4	86
164	Prolactin signaling through focal adhesion complexes is amplified by stiff extracellular matrices in breast cancer cells. Oncotarget, 2016, 7, 48093-48106.	0.8	20
165	Highly aligned stromal collagen is a negative prognostic factor following pancreatic ductal adenocarcinoma resection. Oncotarget, 2016, 7, 76197-76213.	0.8	163
166	A subset of myofibroblastic cancer-associated fibroblasts regulate collagen fiber elongation, which is prognostic in multiple cancers. Oncotarget, 2016, 7, 6159-6174.	0.8	149
167	Abstract 4394: Phenotypic heterogeneity of disseminated tumor cells is predetermined by primary tumor hypoxic microenvironments. , 2016, , .		Ο
168	Development of a Bioinspired Stroma Model to Study the Role of Collagen Topology in Pancreatic Ductal Adenocarcinoma. Microscopy and Microanalysis, 2015, 21, 87-88.	0.2	0
169	The ImageJ ecosystem: An open platform for biomedical image analysis. Molecular Reproduction and Development, 2015, 82, 518-529.	1.0	2,029
170	OptogenSIM: a 3D Monte Carlo simulation platform for light delivery design in optogenetics. Biomedical Optics Express, 2015, 6, 4859.	1.5	54
171	Tumor mechanics and metabolic dysfunction. Free Radical Biology and Medicine, 2015, 79, 269-280.	1.3	95
172	Multi-functional self-fluorescent unimolecular micelles for tumor-targeted drug delivery and bioimaging. Biomaterials, 2015, 47, 41-50.	5.7	96
173	Patterned Optogenetic Modulation of Neurovascular and Metabolic Signals. Journal of Cerebral Blood Flow and Metabolism, 2015, 35, 140-147.	2.4	15
174	Endogenous Optical Signals Reveal Changes of Elastin and Collagen Organization During Differentiation of Mouse Embryonic Stem Cells. Tissue Engineering - Part C: Methods, 2015, 21, 995-1004.	1.1	13
175	Matrix metalloproteinase 9 modulates collagen matrices and wound repair. Development (Cambridge), 2015, 142, 2136-2146.	1.2	111
176	Closed-Loop Optogenetic Brain Interface. IEEE Transactions on Biomedical Engineering, 2015, 62, 2327-2337.	2.5	46
177	Multi-view second-harmonic generation imaging of mouse tail tendon via reflective micro-prisms. Optics Letters, 2015, 40, 3201.	1.7	6
178	Periductal stromal collagen topology of pancreatic ductal adenocarcinoma differs from that of normal and chronic pancreatitis. Modern Pathology, 2015, 28, 1470-1480.	2.9	110
179	Non-line-of-sight imaging using a time-gated single photon avalanche diode. Optics Express, 2015, 23, 20997.	1.7	194
180	Anthocyanin Vacuolar Inclusions Form by a Microautophagy Mechanism. Plant Cell, 2015, 27, 2545-2559.	3.1	153

#	Article	IF	CITATIONS
181	Abstract 3000: Hypoxic primary tumor stress microenvironments prime DTCs in lungs for dormancy. Cancer Research, 2015, 75, 3000-3000.	0.4	2
182	Dense Collagen-I Matrices Enhance Pro-Tumorigenic Estrogen-Prolactin Crosstalk in MCF-7 and T47D Breast Cancer Cells. PLoS ONE, 2015, 10, e0116891.	1.1	48
183	Abstract B02: Matrix stiffness regulates local metabolism of breast carcinoma cells. , 2015, , .		1
184	Exposure to Optogenetic Blue Light Attenuates Inflammatory Gene Expression in Nonâ€ŧransgenic Murine Microglia. FASEB Journal, 2015, 29, 835.5.	0.2	0
185	Matrix metalloproteinase 9 modulates collagen matrices and wound repair. Journal of Cell Science, 2015, 128, e1.1-e1.1.	1.2	1
186	Abstract 332: Extracellular matrix stiffness regulates metabolic state in metastatic, but not quiescent, breast carcinoma cells. , 2015, , .		0
187	Characterization of Fibrillar Collagens and Extracellular Matrix of Glandular Benign Prostatic Hyperplasia Nodules. PLoS ONE, 2014, 9, e109102.	1.1	71
188	A Three-Dimensional Computational Model of Collagen Network Mechanics. PLoS ONE, 2014, 9, e111896.	1.1	63
189	The effect of micro-ECoG substrate footprint on the meningeal tissue response. Journal of Neural Engineering, 2014, 11, 046011.	1.8	63
190	Experimental and simulation study of the wavelength dependent second harmonic generation of collagen in scattering tissues. Optics Letters, 2014, 39, 1897.	1.7	29
191	3D Collagen Alignment Limits Protrusions to Enhance Breast Cancer Cell Persistence. Biophysical Journal, 2014, 107, 2546-2558.	0.2	346
192	A chronic window imaging device for the investigation of in vivo peripheral nerves. , 2014, 2014, 1985-8.		1
193	Extraction of optical properties and prediction of light distribution in rat brain tissue. Journal of Biomedical Optics, 2014, 19, 075001.	1.4	57
194	BI-24 * COLLAGEN PLAYS A ROLE IN GLIOBLASTOMA TUMOR INVASION AND PATIENT SURVIVAL. Neuro-Oncology, 2014, 16, v28-v28.	0.6	0
195	Cooperativity among Rev-Associated Nuclear Export Signals Regulates HIV-1 Gene Expression and Is a Determinant of Virus Species Tropism. Journal of Virology, 2014, 88, 14207-14221.	1.5	23
196	MP36-04 QUANTIFICATION OF RENAL CELL OPTICAL BIOMARKERS USING SECOND HARMONIC GENERATION IMAGING. Journal of Urology, 2014, 191, .	0.2	0
197	Computational segmentation of collagen fibers from second-harmonic generation images of breast cancer. Journal of Biomedical Optics, 2014, 19, 016007.	1.4	294
198	Laser Scanning Confocal Microscopy: History, Applications, and Related Optical Sectioning Techniques. Methods in Molecular Biology, 2014, 1075, 9-47.	0.4	58

#	Article	IF	CITATIONS
199	Advanced materials for neural surface electrodes. Current Opinion in Solid State and Materials Science, 2014, 18, 301-307.	5.6	21
200	A microfluidic coculture and multiphoton FAD analysis assay provides insight into the influence of the bone microenvironment on prostate cancer cells. Integrative Biology (United Kingdom), 2014, 6, 627-635.	0.6	31
201	Calsyntenin-1 Regulates Axon Branching and Endosomal Trafficking during Sensory Neuron Development In Vivo. Journal of Neuroscience, 2014, 34, 9235-9248.	1.7	54
202	Second-harmonic generation imaging of cancer. Methods in Cell Biology, 2014, 123, 531-546.	0.5	73
203	SORCS1 is necessary for normal insulin secretory granule biogenesis in metabolically stressed β cells. Journal of Clinical Investigation, 2014, 124, 4240-4256.	3.9	53
204	Automated quantification of aligned collagen for human breast carcinoma prognosis. Journal of Pathology Informatics, 2014, 5, 28.	0.8	172
205	Abstract 1116: Response to cyclooxygenase-2 inhibition is regulated by collagen dense stroma. , 2014, , .		Ο
206	OpenSPIM: an open-access light-sheet microscopy platform. Nature Methods, 2013, 10, 598-599.	9.0	312
207	1069 MULTIPHOTON MICROSCOPIC CHARACTERIZATION OF RENAL CELL CARCINOMA. Journal of Urology, 2013, 189, .	0.2	0
208	Association of cellular and molecular responses in the rat mammary gland to 17β-estradiol with susceptibility to mammary cancer. BMC Cancer, 2013, 13, 573.	1.1	19
209	A bioengineered heterotypic stroma–cancer microenvironment model to study pancreatic ductal adenocarcinoma. Lab on A Chip, 2013, 13, 3965.	3.1	51
210	ECM-Incorporated Hydrogels Cross-Linked via Native Chemical Ligation To Engineer Stem Cell Microenvironments. Biomacromolecules, 2013, 14, 3102-3111.	2.6	30
211	The collagen receptor discoidin domain receptor 2 stabilizes SNAIL1 to facilitate breast cancer metastasis. Nature Cell Biology, 2013, 15, 677-687.	4.6	312
212	Spatial and Temporal Analysis of Extracellular Matrix Proteins in the Developing Murine Heart: A Blueprint for Regeneration. Tissue Engineering - Part A, 2013, 19, 1132-1143.	1.6	65
213	Nonlinear optical microscopy and ultrasound imaging of human cervical structure. Journal of Biomedical Optics, 2013, 18, 031110.	1.4	54
214	Image-inspired 3D multiphoton excited fabrication of extracellular matrix structures by modulated raster scanning. Optics Express, 2013, 21, 25346.	1.7	28
215	Simultaneous determination of the second-harmonic generation emission directionality and reduced scattering coefficient from three-dimensional imaging of thick tissues. Journal of Biomedical Optics, 2013, 18, 116008.	1.4	18
216	RhoA is down-regulated at cell–cell contacts via p190RhoGAP-B in response to tensional homeostasis. Molecular Biology of the Cell, 2013, 24, 1688-1699.	0.9	27

#	Article	IF	CITATIONS
217	A shift in energy metabolism anticipates the onset of sarcopenia in rhesus monkeys. Aging Cell, 2013, 12, 672-681.	3.0	66
218	Stiff Collagen Matrices Increase Tumorigenic Prolactin Signaling in Breast Cancer Cells. Journal of Biological Chemistry, 2013, 288, 12722-12732.	1.6	112
219	Hyperspectral Multi-Point Confocal Microscope. , 2013, , .		1
220	Abstract A35: Aligned collagen is a prognostic signature for survival in human breast carcinoma. , 2013, , .		4
221	Abstract 4960: COX-2 inhibition with celecoxib delays the progression of invasive mammary carcinoma in a murine model of collagen dense stroma , 2013, , .		Ο
222	Goniometric measurements of thick tissue using Monte Carlo simulations to obtain the single scattering anisotropy coefficient. Biomedical Optics Express, 2012, 3, 2707.	1.5	39
223	Second-harmonic generation and fluorescence lifetime imaging microscopy through a rodent mammary imaging window. Proceedings of SPIE, 2012, , .	0.8	2
224	Registration of multiphoton optical images of cervical tissue to quantitative ultrasound data. , 2012, ,		1
225	Microtubules regulate GEF-H1 in response to extracellular matrix stiffness. Molecular Biology of the Cell, 2012, 23, 2583-2592.	0.9	78
226	Three-Dimensional Surface Profile Measurement of Microlenses Using the Shack–Hartmann Wavefront Sensor. Journal of Microelectromechanical Systems, 2012, 21, 530-540.	1.7	14
227	Mesenchymal Stem Cell Interactions with 3D ECM Modules Fabricated via Multiphoton Excited Photochemistry. Biomacromolecules, 2012, 13, 2917-2925.	2.6	35
228	Biological imaging software tools. Nature Methods, 2012, 9, 697-710.	9.0	462
229	A call for bioimaging software usability. Nature Methods, 2012, 9, 666-670.	9.0	116
230	NIH Image to ImageJ: 25 years of image analysis. Nature Methods, 2012, 9, 671-675.	9.0	46,756
231	Fiji: an open-source platform for biological-image analysis. Nature Methods, 2012, 9, 676-682.	9.0	47,818
232	Imaging cardiac extracellular matrices: a blueprint for regeneration. Trends in Biotechnology, 2012, 30, 233-240.	4.9	25
233	Opportunities for multiple-beam synchrotron-based mid-infrared imaging at IRENI. Vibrational Spectroscopy, 2012, 60, 10-15.	1.2	17
234	Cell death, nonâ€invasively assessed by intrinsic fluorescence intensity of NADH, is a predictive indicator of functional differentiation of embryonic stem cells. Biology of the Cell, 2012, 104, 352-364.	0.7	21

#	Article	IF	CITATIONS
235	Endogenous Fluorescence Signatures in Living Pluripotent Stem Cells Change with Loss of Potency. PLoS ONE, 2012, 7, e43708.	1.1	17
236	Transition to invasion in breast cancer: a microfluidic in vitro model enables examination of spatial and temporal effects. Integrative Biology (United Kingdom), 2011, 3, 439-450.	0.6	201
237	Resveratrol Metabolites Do Not Elicit Early Pro-apoptotic Mechanisms in Neuroblastoma Cells. Journal of Agricultural and Food Chemistry, 2011, 59, 4979-4986.	2.4	37
238	Postpartum mammary gland involution drives progression of ductal carcinoma in situ through collagen and COX-2. Nature Medicine, 2011, 17, 1109-1115.	15.2	318
239	Aligned Collagen Is a Prognostic Signature for Survival in Human Breast Carcinoma. American Journal of Pathology, 2011, 178, 1221-1232.	1.9	1,026
240	Structural changes in mixed Col I/Col V collagen gels probed by SHG microscopy: implications for probing stromal alterations in human breast cancer. Biomedical Optics Express, 2011, 2, 2307.	1.5	78
241	Fast localized wavefront correction using area-mapped phase-shift interferometry. Optics Letters, 2011, 36, 2892.	1.7	3
242	Multiphoton Flow Cytometry to Assess Intrinsic and Extrinsic Fluorescence in Cellular Aggregates: Applications to Stem Cells. Microscopy and Microanalysis, 2011, 17, 540-554.	0.2	18
243	Quantification of Collagen Organization and Extracellular Matrix Factors within the Healing Ligament. Microscopy and Microanalysis, 2011, 17, 779-787.	0.2	39
244	338: Detection of cervical collagen with quantitative ultrasound. American Journal of Obstetrics and Gynecology, 2011, 204, S138.	0.7	0
245	A nondenatured, noncrosslinked collagen matrix to deliver stem cells to the heart. Regenerative Medicine, 2011, 6, 569-582.	0.8	29
246	Surface profiling and characterization of microlenses utilizing a Shack-Hartmann wavefront sensor. , 2011, , .		0
247	Three-dimensional surface profiling and optical characterization of liquid microlens using a Shack–Hartmann wave front sensor. Applied Physics Letters, 2011, 98, 171104.	1.5	19
248	Improved structure, function and compatibility for CellProfiler: modular high-throughput image analysis software. Bioinformatics, 2011, 27, 1179-1180.	1.8	948
249	Abstract 4749: Aligned collagen is a prognostic signature for survival in human breast carcinoma. , 2011, , .		0
250	Visualization of Morphological and Molecular Features Associated with Chronic Ischemia in Bioengineered Human Skin. Microscopy and Microanalysis, 2010, 16, 117-131.	0.2	2
251	Bimolecular fluorescence complementation analysis of eukaryotic fusion products. Biology of the Cell, 2010, 102, 525-537.	0.7	10
252	CGEF-1 and CHIN-1 Regulate CDC-42 Activity during Asymmetric Division in the <i>Caenorhabditis elegans</i> Embryo. Molecular Biology of the Cell, 2010, 21, 266-277.	0.9	105

#	Article	IF	CITATIONS
253	Detecting cervical microstructure via ultrasound and optical microscopy. , 2010, , .		8
254	Engineering Threeâ€Đimensional Collagen Matrices to Provide Contact Guidance during 3D Cell Migration. Current Protocols in Cell Biology, 2010, 47, Unit 10.17.	2.3	29
255	Metadata matters: access to image data in the real world. Journal of Cell Biology, 2010, 189, 777-782.	2.3	858
256	Chapter 3. Screening Approaches for Stem Cells. , 2010, , 45-80.		0
257	Nonlinear optical microscopy and computational analysis of intrinsic signatures in breast cancer. , 2009, 2009, 4077-80.		12
258	Image reconstruction of multiphoton microscopy data. , 2009, , 803-806.		0
259	Unifying biological image formats with HDF5. Communications of the ACM, 2009, 52, 42-47.	3.3	39
260	Filamin A–β1 Integrin Complex Tunes Epithelial Cell Response to Matrix Tension. Molecular Biology of the Cell, 2009, 20, 3224-3238.	0.9	103
261	Open source bioimage informatics for cell biology. Trends in Cell Biology, 2009, 19, 656-660.	3.6	47
262	Shining new light on 3D cell motility and the metastatic process. Trends in Cell Biology, 2009, 19, 638-648.	3.6	56
263	Multiphoton microscopy and fluorescence lifetime imaging microscopy (FLIM) to monitor metastasis and the tumor microenvironment. Clinical and Experimental Metastasis, 2009, 26, 357-370.	1.7	185
264	Fluorescence Lifetime Imaging of Endogenous Fluorophores in Histopathology Sections Reveals Differences Between Normal and Tumor Epithelium in Carcinoma In Situ of the Breast. Cell Biochemistry and Biophysics, 2009, 53, 145-157.	0.9	125
265	Matrix density-induced mechanoregulation of breast cell phenotype, signaling and gene expression through a FAK–ERK linkage. Oncogene, 2009, 28, 4326-4343.	2.6	557
266	Integrated studies of biology: multiplexed imaging assays from molecules to man and back. Current Opinion in Biotechnology, 2009, 20, 1-3.	3.3	119
267	Control of 3-dimensional collagen matrix polymerization for reproducible human mammary fibroblast cell culture in microfluidic devices. Biomaterials, 2009, 30, 4833-4841.	5.7	138
268	Bioimage Informatics for Experimental Biology. Annual Review of Biophysics, 2009, 38, 327-346.	4.5	98
269	Collagen density promotes mammary tumor initiation and progression. BMC Medicine, 2008, 6, 11.	2.3	1,129
270	Contact Guidance Mediated Three-Dimensional Cell Migration is Regulated by Rho/ROCK-Dependent Matrix Reorganization. Biophysical Journal, 2008, 95, 5374-5384.	0.2	426

#	Article	IF	CITATIONS
271	Mammary Epithelial-Specific Disruption of Focal Adhesion Kinase Retards Tumor Formation and Metastasis in a Transgenic Mouse Model of Human Breast Cancer. American Journal of Pathology, 2008, 173, 1551-1565.	1.9	126
272	Nonlinear Optical Imaging of Cellular Processes in Breast Cancer. Microscopy and Microanalysis, 2008, 14, 532-548.	0.2	56
273	Student Learning of Early Embryonic Development via the Utilization of Research Resources from the Nematode <i>Caenorhabditis elegans</i> . CBE Life Sciences Education, 2008, 7, 64-73.	1.1	9
274	Nonlinear optical imaging and spectral-lifetime computational analysis of endogenous and exogenous fluorophores in breast cancer. Journal of Biomedical Optics, 2008, 13, 031220.	1.4	52
275	<i>In vivo</i> multiphoton microscopy of NADH and FAD redox states, fluorescence lifetimes, and cellular morphology in precancerous epithelia. Proceedings of the National Academy of Sciences of the United States of America, 2007, 104, 19494-19499.	3.3	898
276	In vivo multiphoton fluorescence lifetime imaging of protein-bound and free nicotinamide adenine dinucleotide in normal and precancerous epithelia. Journal of Biomedical Optics, 2007, 12, 024014.	1.4	317
277	WormClassroom.org: An Inquiry-rich Educational Web Portal for Research Resources of Caenorhabditis elegans. CBE Life Sciences Education, 2007, 6, 98-108.	1.1	7
278	Cortical granule exocytosis in <i>C. elegans</i> is regulated by cell cycle components including separase. Development (Cambridge), 2007, 134, 3837-3848.	1.2	98
279	Lrrc10 is required for early heart development and function in zebrafish. Developmental Biology, 2007, 308, 494-506.	0.9	33
280	BioClips of symmetric and asymmetric cell division. Biology of the Cell, 2007, 99, 289-295.	0.7	2
281	Visualization approaches for multidimensional biological image data. BioTechniques, 2007, 43, S31-S36.	0.8	40
282	Applications of combined spectral lifetime microscopy for biology. BioTechniques, 2006, 41, 249-257.	0.8	32
283	VisBio: a Flexible Open-Source Visualization Package for Multidimensional Image Data. Microscopy Today, 2006, 14, 6-11.	0.2	0
284	Collagen reorganization at the tumor-stromal interface facilitates local invasion. BMC Medicine, 2006, 4, 38.	2.3	1,417
285	In vivo Multiphoton Fluorescence Lifetime Imaging of Free and Protein-bound NADH in Normal and Pre-cancerous Epithelia. , 2006, , .		1
286	Wavelet Compression of Three-Dimensional Time-Lapse Biological Image Data. Microscopy and Microanalysis, 2005, 11, 9-17.	0.2	3
287	Tools for Visualizing Multidimensional Images from Living Specimens. Photochemistry and Photobiology, 2005, 81, 1116.	1.3	33
288	Multiphoton Microscopy of Endogenous Fluorescence Differentiates Normal, Precancerous, and Cancerous Squamous Epithelial Tissues. Cancer Research, 2005, 65, 1180-1186.	0.4	214

#	Article	IF	CITATIONS
289	Metabolic Mapping of MCF10A Human Breast Cells via Multiphoton Fluorescence Lifetime Imaging of the Coenzyme NADH. Cancer Research, 2005, 65, 8766-8773.	0.4	351
290	VisBio: A Computational Tool for Visualization of Multidimensional Biological Image Data. Traffic, 2004, 5, 411-417.	1.3	33
291	Molecular Expressions: Exploring the World of Optics and Microscopy http:microscopy.fsu.edu. Biology of the Cell, 2004, 96, 403-405.	0.7	2
292	Simultaneous two-photon spectral and lifetime fluorescence microscopy. Applied Optics, 2004, 43, 5173.	2.1	98
293	Analysis of histology specimens using lifetime multiphoton microscopy. Journal of Biomedical Optics, 2003, 8, 376.	1.4	42
294	Optical workstation with concurrent, independent multiphoton imaging and experimental laser microbeam capabilities. Review of Scientific Instruments, 2003, 74, 193-201.	0.6	54
295	Applying Multiphoton Imaging to the Study of Membrane Dynamics in Living Cells. Traffic, 2001, 2, 775-780.	1.3	29
296	Sonification of hyperspectral fluorescence microscopy datasets. F1000Research, 0, 5, 2572.	0.8	0